Hybrid diagnostic agent system for the fast-breeder reactor "Monju"

GOFUKU Akio[1], TAKAHASHI Makoto[2], NAGAMATSU Takashi[3], MOCHIZUKI Hiroyasu[4], FURUSAWA Hiroaki[1], and MINOWA Hirotsugu[1]

1. *Graduate School of Natural Science and Technology, Okayama University, 3-1-1 Tsushima-Naka, Kita-ku, Okayama 700-8530, Japan (fukuchan@sys.okayama-u.ac.jp)*
2. *Graduate School of Engineering, Tohoku University, 6-6 Aramaki-Aoba, Aoba-ku, Sendai, Miyagi 980-8579, Japan*
3. *Graduate School of Maritime Sciences, Kobe University, 5-1-1 Fukaeminami-machi, Higashinada-ku, Kobe 658-0022, Japan*
4. *Research Institute of Nuclear Engineering, University of Fukui, 1-2-4 Kanawa-cho, Tsuruga 914-0055, Japan*

Abstract: A hybrid diagnostic agent system is developed to detect and identify early an anomaly that might happen in the fast-breeder reactor "Monju". The system outputs a diagnostic result by integrating the results of diagnosis by four diagnostic software agents. They are (1) an estimation agent of overall heat transfer coefficient of evaporator and superheater, (2) a state identification agent based on SVM (Support Vector Machine), (3) an anomaly detection agent by WT (Wavelet Transformation), and (4) a CBR (Case-Based Reasoning) agent using several attributes in both time and frequency domains. This article describes the four diagnostic techniques and the hybrid diagnostic agent system.
Keyword: diagnostic system; fast-breeder reactor; hybrid agent system

1 Introduction

"Monju" is a sodium-cooled fast-breeder reactor (FBR), its first achievement being effected in April 1994. It was however operated for only a short period of time, owing to the sodium leak accident that occurred in December 1995 and some troubles. The improvement and renewal of its systems are made in order to continue experiments that yield various data for the development of commercial plants.

Fast-breeder reactor uses liquid sodium as coolant; it is therefore necessary to handle liquid sodium with caution due to its chemical characteristics. This means that some improved diagnostic systems to detect a small leakage of sodium coolant to water-steam loop and small anomalies in system components are pivotal. The Japan Atomic Energy Agency (JAEA) already developed a "Monju" distributed diagnostic agent system [1] in 2001 to diagnose anomalies that might happen in "Monju". It was equipped with various types of diagnostic sub-systems applying state-of-the-art techniques at the time.

The Japanese government promoted R&D activities aimed at developing improved diagnostic systems for "Monju", by applying new and/or developing techniques in signal processing and artificial intelligence. The authors studied a four-year R&D project from December 2009 to March 2013. The purpose of the project was to develop a hybrid diagnostic technique that integrates several diagnostic techniques by the use of "Monju" process signals, and implement it as a hybrid diagnostic agent system in the "Monju" distributed diagnostic agent system. The developed agent system comprises several diagnostic agents, and a diagnostic result is given by integrating the results of the diagnostic agents.

This article describes the diagnostic techniques examined by our four-year project, an integration technique of the results given by the diagnostic techniques and the implementation of the hybrid diagnostic technique as an agent system for the "Monju" distributed diagnostic agent system.

2 Preparation of process signal data for applicability evaluation

2.1 Approach of preparation of process signal data

The applicability of the developed diagnostic techniques is evaluated by using two types of artificial process signal data. The first type is the data that

Received date: July 3, 2013
(Revised date: July 9, 2013)

imitate "Monju" process signals in small anomalies by superimposing artificial noise data to the trend data obtained by numerical simulations. The second type is a set of vibration/acoustic signal data generated by small experimental equipment.

2.2 Numerical simulation by a thermal-hydraulics analysis code

The time-response data of "Monju" process signals at several minor anomalies are obtained by a thermal-hydraulic simulation code NETFLOW++ [2]. Five types of anomalies are considered in the simulations: (1) a small decrease of feedwater flow rate, (2) a small decrease of heat transfer rate in the evaporator, (3) a small decrease of primary sodium flow rate, (4) a small increase of main steam pressure, and (5) a small decrease of feedwater temperature.

The whole simulation model of the "Monju" system is shown in Fig. 1. As shown in the figure, the model consists of three primary and secondary sodium loops, a water-steam system, a main steam control valve, a high pressure turbine, a low pressure turbine, a condenser, feedwater heaters, a feedwater pump, a deaerator, three feedwater valves for three loops, and so on. The geometrical data are estimated from "Monju" construction application documents and open data in the Web pages of JAEA. The data of feedwater heaters are estimated from a thermal power station in almost the same electric power generation.

As examples of simulation results, Fig. 2 shows the time responses of some major state variables in the case of an anomaly of A-loop feedwater control valve at 40% electric power. The feedwater flow rate decreases about 10% by the occurrence of the anomaly at 1000 [**s**]. Due to the anomaly, the steam temperature at the outlet of A-loop evaporator increases and reaches at the temperature that initiates a scram signal at 2100 [**s**]. The outlet temperatures of the evaporators in other loops are almost constant. However, the temperature increase causes the temperature increase of A-loop secondary sodium at the outlet of evaporator as shown in Fig. 2 (b).

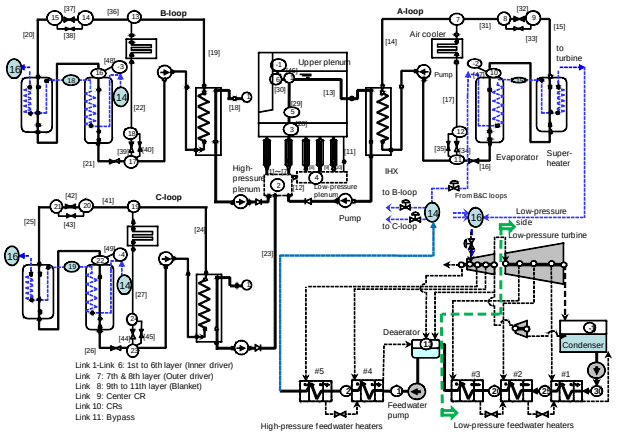

Fig. 1 Simulation model of "Monju".

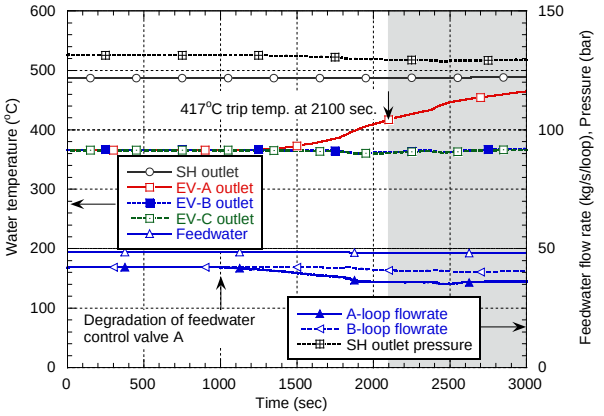

(a) Water-steam side

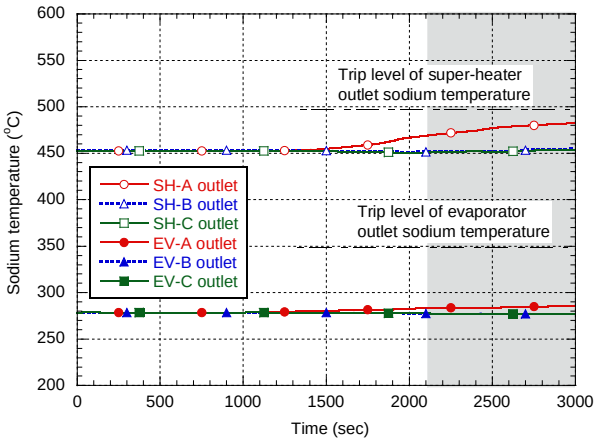

(b) Secondary sodium side

Fig. 2 Time responses of major state variables in the case of an anomaly at A-loop feedwater control valve.

2.3 Generation of imitated "Monju" process signals

To prepare process signal data, the characteristics of "Monju" process signals measured in an experimental operation at 40% electric power are first analyzed by FFT (Fast Fourier Transform) analysis. An AR (Autoregressive) model is identified for each process

signal to express the characteristics of its noises. Artificial noises are generated based on the AR models. The "Monju" process signal data at the anomalies are imitated by superimposing the artificial noises to the time-response data simulated by a thermal-hydraulic simulation code NETFLOW++ for several anomalies.

2.4 Vibration and acoustic signals by small pump equipment

Vibration and acoustic signal data are obtained by experimental equipment with two water loops. The signal data obtained by the equipment are used to evaluate the applicability of an anomaly detection technique by WT (Wavelet Transform). The appearance of the equipment is shown in Fig. 3. There are two parallel water lines. Each water line is composed of a centrifugal-type pump, a flow meter, and a manual valve to introduce a small amount of air.

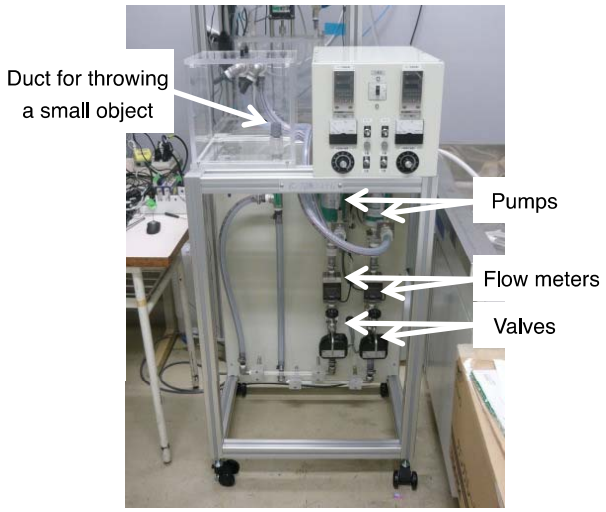

Fig. 3 Water loop experimental equipment.

Some anomalies in the pump are considered. The ceramic axis in one of the pumps has a small artificial flaw. Each shuttlecock of the centrifugal-type pump can install a small screw to imitate unbalanced rotation conditions of a pump. There is a duct to introduce a small obstacle in the loop with a normal pump. Four types of small obstacles with different geometrical shapes are prepared.

3 Diagnostic techniques for small anomalies

3.1 Diagnostic techniques developed

The authors developed four diagnostic techniques to detect small anomalies using process signals. They are: (1) an estimation technique of overall heat transfer coefficient of evaporator and superheater, (2) a state identification technique based on SVM (Support Vector Machine), (3) an anomaly detection technique by WT, and (4) a CBR (Case-Based Reasoning) diagnostic technique using several attributes in both time and frequency domains. In the following sub-sections, the outline of each diagnostic technique is described.

3.2 Estimation technique of overall heat transfer coefficients of evaporator and superheater

Diagnostic techniques of evaporator and superheater using observed process signals are developed to monitor their operation conditions [3]. The techniques estimate the overall heat transfer coefficients (that are important unobserved state variables for evaporator and superheater) based on their simplified mathematical models.

Simplified models of the evaporator and superheater of "Monju" are constructed, as shown in Figs. 4 and 5, by considering their structures, the flows of secondary sodium and water/steam, and small number of process signals available to estimate the overall heat transfer coefficients. In the models, the heat transfers from evaporator and superheater to the gas around them are ignored. The inner volume of the evaporator tubes and cylindrical vessel is divided into compressed water region, saturated water/steam region and superheated steam region depending on the state of water. The overall heat transfer coefficient in the saturated water/steam region of evaporator is assumed to be calculated from the overall heat transfer coefficients in compressed water and superheated steam regions, considering the volumetric qualities of saturated water and steam in saturation region. All steam flowing into superheater is assumed to be superheated steam.

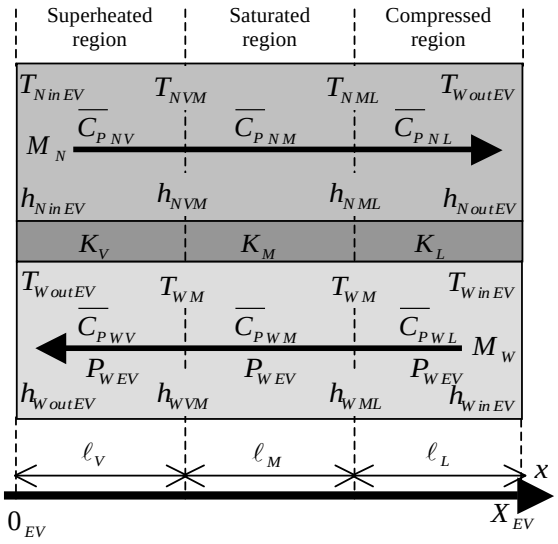

Fig.4 Schematic of a simplified model of evaporator.

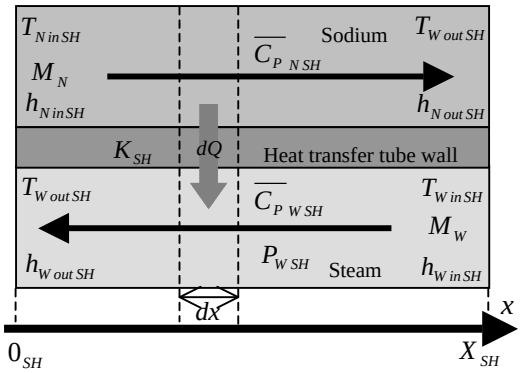

Fig.5 Schematic of a simplified model of superheater.

In the models, the variables and subscripts mean as follows:

Variable

$\overline{C_P}$: Average specific heat under constant pressure,
M : Mass flow rate,
T : Temperature,
P : Pressure,
h : Specific enthalpy,
X : Length of heat transfer tube,
R : Circumferential length of heat transfer tube,
A : Heat transfer area in minute length dx,
Q : Total amount of heat transfer,
K : Overall heat transfer coefficient,
λ : Thermal conductivity,
d : Thickness of heat transfer tube,

Subscript

SH : Superheater,
EV : Evaporator,
N : Secondary sodium,
W : Water/steam,
V : Superheated steam region in evaporator,
M : Saturated water/steam region in evaporator,
L : Compressed water region in evaporator,
in : Inlet,
out : Outlet,
0 : Position at $x = 0$,
VM : Boundary between superheated steam region and saturated water/steam region in evaporator,
ML : Boundary between saturated water/steam region and compressed water region in evaporator,

Based on the simplified models, the following equations to calculate overall heat transfer coefficients of evaporator and superheater are derived:

$$K_V = \frac{K_{SH}\lambda_{SH}\lambda_V}{\lambda_{SH}\lambda_V - K_{SH}\lambda_V d_{SH} + K_{SH}\lambda_{SH} d_V} \tag{1}$$

$$K_M = \frac{aK_V + bK_L}{a+b} = \frac{aK_V + bK_L}{c} \tag{2}$$

$$K_L = \frac{-K_V\left(aA_{allEV}K_V - a\alpha_1 - b\alpha_2 - c\alpha_3\right) + K_V\sqrt{Z}}{2b\left(A_{allEV}K_V - \alpha_1\right)} \tag{3}$$

$$Z = \left(aA_{allEV}K_V - a\alpha_1 - b\alpha_2 - c\alpha_3\right)^2 + 4ab\alpha_2\left(A_{allEV}K_V - \alpha_1\right) \tag{4}$$

$$K_{SH} = \frac{M_W\left(h_{WoutSH} - h_{WinSH}\right)\left(\log\Delta T_{X_{SH}} - \log\Delta T_{0SH}\right)}{A_{allSH}\left(\Delta T_{X_{SH}} - \Delta T_{0SH}\right)} \tag{5}$$

As an example to estimate the overall heat transfer coefficient, Fig. 6 shows estimation results in the case of a decrease of heat transfer rate in evaporator. The figure also shows the time responses of confidence value; a descriptor of the certainty of anomaly detection. The anomaly happens at 1000 [**s**]. Owing to the occurrence of the anomaly, the overall heat

transfer coefficient in the evaporator decreases while that in the superheater increases. The confidence value in condition monitoring of evaporator becomes 1.0 after 13 seconds due to the anomaly. On the other hand, the confidence value for the superheater diagnosis becomes 1.0 after 86 seconds due to the occurrence of the anomaly. Moreover, a drastic drop in the confidence value is observed, since the overall heat transfer coefficient slightly decreases by increasing the temperature difference between the inlet steam of superheater and outlet sodium of superheater when the anomaly happens. Finally, the confidence value becomes 1.0 by the gradual increase of the overall heat transfer coefficient due to the decrease of the temperature difference.

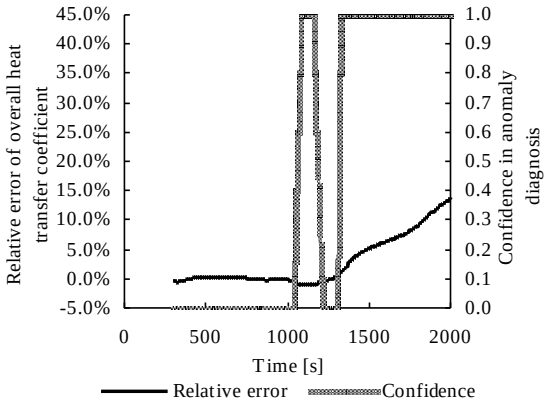

(a) Superheater

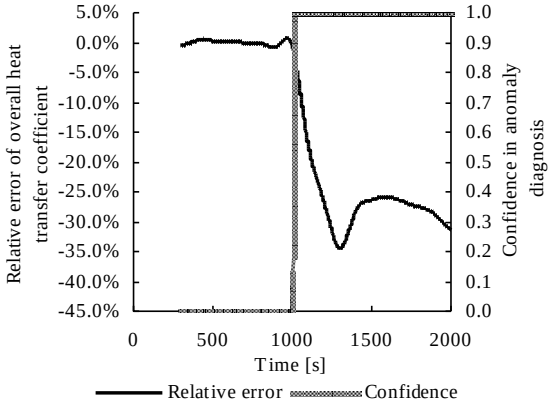

(b) Evaporator

Fig. 6 Estimation results of overall heat transfer coefficients.

3.3 State identification technique based on support vector machine

The SVM is a kind of machine learning technique and is widely applied to construct a state identifier [4, 5]. The SVM has a characteristic feature to derive nonlinear identification functions from training data. It can update the identification functions when new training data are obtained.

In general, the performance of a diagnosis technique becomes high if suitable set of process signals is selected. The derivation of nonlinear functions for a SVM using all process signals needs much computation power. Therefore, a technique to select a set of process signals that give high diagnostic performance is crucial for the SVM in diagnostic applications. The authors develop a signal selection technique for a state identifier applying the SVM.

The performance of state diagnosis is measured by an index called "model score". The model score M is calculated by

$$M = \frac{1}{2}\left(\frac{n_{An}}{n_{Sn}} + \frac{n_{Aa}}{n_{Sa}}\right) \tag{6}$$

where n_{Sn} and n_{Sa} are numbers of samples in normal state and abnormal state, and n_{An} and n_{Aa} are numbers of correctly identified samples in normal state and abnormal state, respectively.

The signal selection technique developed is outlined as follows:

Step 1: Selection of useful signals.

Step 1.1: Calculate a base model score M_B of the SVM state identifier using all process signals.

Step 1.2: Calculate model score M_i of the SVM state identifier using a process signal i.

Step 1.3: Select the signal if the model score of the SVM identifier using the signal is higher than M_B or the order of the model score in arranging model scores from the highest is smaller than a predetermined order. The number of selected signals is set to m.

Step 2: Optimization of signal combination.

Step 2.1: Obtaining the set of signal combinations by using the signals selected in Step 1.

Step 2.2: For a given j (initially 2), construct ${}_mC_j$ SVM state identifiers using j signals and calculate their model scores.

Step 2.3: Construct an SVM predictor to estimate the model scores of SVM state identifiers using $j+1$ signals from the model scores of SVM state

identifiers using 1 to j signals and estimate the model scores $M_k^{E(j+1)}$ of SVM state identifiers using $j+1$ signals.

Step 2.4: Construct ${}_mC_{j+1}$ SVM state identifiers using $j+1$ signals and calculate their model scores $M_k^{C(j+1)}$.

Step 2.5: Move to Step 2.6 if the following condition is satisfied. Otherwise, return Step 2.2 after incrementing j. The condition is that the subtraction from the average of $M_k^{E(j+1)}$ and the average of $M_k^{C(j+1)}$ is smaller than a predetermined threshold value T_A and the covariance of $M_k^{C(j+1)}$ is smaller than a predetermined threshold value T_C.

Step 2.6: Estimate the model scores of SVM state identifiers using $j+1$ to m signals by the SVM predictor.

Step 2.7: Select the SVM state identifier that gives maximum estimated or calculated model scores.

Table 1 Performance comparison of anomaly detection

No.	Anomaly that happened	Optimized SVM	SVM using all signals
	Selected process signals		
1	small decrease of feedwater flow rate	50 [**s**]	582 [**s**]
	Main steam pressure Secondary Na temperature at the outlet of evaporator		
2	small decrease of heat transfer rate in the evaporator	31 [**s**]	31 [**s**]
	Steam temperature at the inlet of superheater Feedwater flow rate Secondary Na temperature at the outlet of superheater Steam temperature at the outlet of evaporator Steam temperature at the outlet of superheater		
3	small decrease of primary sodium flow rate	173 [**s**]	158 [**s**]
	Secondary Na temperature at the inlet of superheater Water temperature at the inlet of evaporator Main steam pressure Primary Na temperature at the outlet of reactor vessel Steam temperature at the outlet of superheater		
4	small decrease of feedwater temperature	46 [**s**]	40 [**s**]
	Water pressure at the inlet of evaporator Feedwater flow rate Secondary Na temperature at the outlet of evaporator Steam pressure at the outlet of evaporator		

The applicability of the signal selection technique is evaluated by comparing the model scores between the SVM state identifiers using all process signals and those using selected process signals for the anomaly cases described in subsection 2.2. The imitated "Monju" process signals described in subsection 2.3 are used. The state identification results are shown in Table 1. The table shows the detection time after the anomaly happens. As shown in the table, almost comparative anomaly detection performance is obtained for the cases 2 to 4, by using several process signals among 16 process signals. In case 1, the detection of the optimized SVM detects the anomaly much faster than the SVM incorporating all signals. The optimized SVM detects the occurrence of the anomaly at 50 [**s**], and diagnoses the plant condition to be normal for about 300 [**s**] after around 250[**s**]. It then again recognizes abnormal plant condition after around 550 [**s**].

3.4 Anomaly detection technique by wavelet transform

A WT has a strong capability to detect the inclusion of a similar wave (short-term change pattern) in a changing signal to a reference wave called a mother wavelet (MW). WT can analyze time-changing data in both frequency and time domains. Therefore, WT is widely applied to detect a sudden anomaly of a component with rotating parts such as pump, motor, and so on. In principle, the detection performance will increase if a mother wavelet is similar to the wave to be detected.

This study develops an anomaly detection technique [6] using a mother wavelet designed from a characteristic wave included in a real signal at an anomaly. To design a mother wavelet from a real signal, this study applies a parasitic discrete wavelet transform (P-DWT) [7] that has a large flexibility in design of a MW and a high processing speed. The decomposition tree of P-DWT is shown in Fig. 7. The "DWT" in the figure means the DWT by multiple resolution analysis using orthogonal MWs. $c_{j,k}$ and $d_{j,k}$ are, respectively, the wavelet coefficient (high frequency components) and scaling factor (low frequency components) obtained by the DWT. x_k^R and x_k^I are the real and image parts of anomaly signal to be detected by the parasitic filter, respectively. $\{u_k^R\}$ and $\{u_k^I\}$ respectively represent the real and image parts of the parasitic filter that approximates a mother wavelet designed from a real signal.

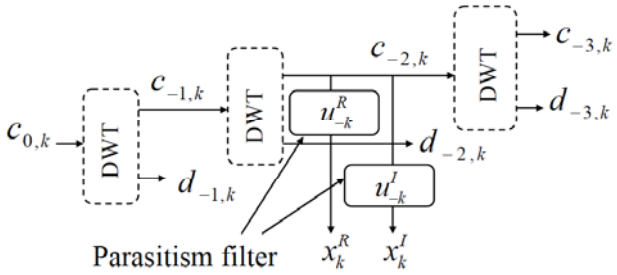

Fig. 7 Decomposition tree of parasitic discrete wavelet transform.

An anomaly is detected by the fast wavelet instantaneous correlation (F-WIC) defined by the following equation:

$$WIC = \sqrt{\left(x_k^R\right)^2 + \left(x_k^I\right)^2} \tag{7}$$

where

$$x_k^R = -\sum_{n=1}^{2^{P+1}} u_n^R c_{j,n-k}, \tag{8}$$

$$x_k^I = -\sum_{n=1}^{2^{P+1}} u_n^I c_{j,n-k}. \tag{9}$$

A similar wave in a signal to the MW is detected if the WIC exceeds a threshold.

As an example of designing MWs from real vibration signals, Fig. 8 shows the real and image parts of parasitic filter made from C-RMW (Complex Real signal Mother Wavelet) for the detection of collision of an acrylic spherical particle to the pump of the small pump equipment. The diameter of the particle is 4.8 [**mm**]. By using the filter, the collision of the spherical particle is successfully detected as shown in Fig. 9. The collision of the particle to the pump is detected at around 2.8 [**s**], as seen from a large value of WIC.

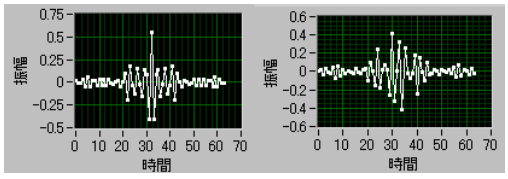

(a) Real part (b) Image part

Fig. 8 Parasitic filter.

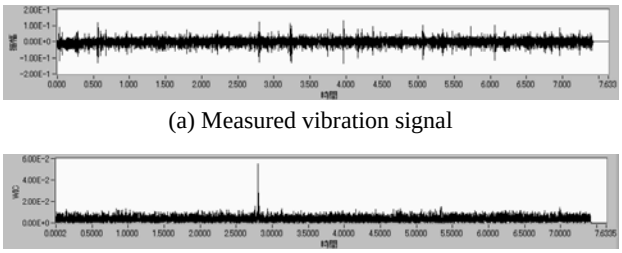

(a) Measured vibration signal

(b) WIC using parasitic filter

Fig. 9 Detection of collision of a spherical particle.

3.5 Case-based reasoning diagnostic technique based on multi-attribute similarity

A diagnostic technique applying case-based reasoning is developed. The characteristic feature of the technique is to use multiple attributes of process signals for similarity evaluation to retrieve a similar case stored in a case base. The structure of the diagnostic technique is shown in Fig. 10. The plant condition is evaluated in the normal condition, if the attributes of process signals are similar to those in the normal condition. If the plant condition is diagnosed to be an anomalous one, the anomaly is identified by comparing the attributes of process signals to those of the anomalous cases. If there is no similar case, the plant condition is diagnosed to be in a different anomalous condition from those of past cases.

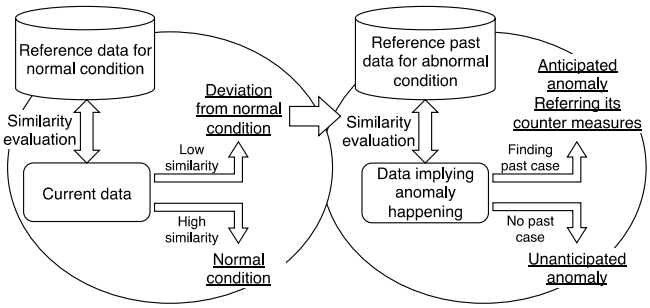

Fig. 10 Structure of case-based reasoning diagnosis system.

In the diagnostic technique, the similarity index is calculated by an exponential distribution-based similarity EDS [8] defined as:

$$EDS = Exp\left(-\frac{|f-g|^n}{S^n}\right), \tag{10}$$

where f and g are N-dimensional attribute vectors and both n and S are matching parameters to adjust the severity of matching. As seen from Eq. (10), EDS approaches 1.0 if the similarity between f and g becomes high. On the other hand, EDS

approaches 0.0 if the similarity between f and g becomes low.

This study uses attributes in both frequency and time domains. In frequency domain, the spectra in low frequency between 0.001 and 0.01 [**Hz**], and high frequency between 0.01 and 0.5 [**Hz**] are utilized. On the other hand, pertinent descriptors such as average, covariance, skewness, and kurtosis are utilized as attributes in time domain. In each process signal, three similarity indices are calculated for the attributes of low and high frequency bands in frequency domain and the attributes in time domain.

As an example of diagnostic results, Fig. 11 shows the trend graphs of similarity indices to normal operating condition. Each curve of the figure shows the mean similarity indices for the process signals detecting the anomaly of a small decrease of feedwater temperature. The anomaly occurs at 10000 [**s**]. As seen from the figure, the similarity indices for the attributes in time domain, the attributes of low and high frequency bands in frequency domain gradually increase from 0.0 to 1.0 after the occurrence of the anomaly. The technique is also confirmed to detect the other anomalies in a short time after their occurrences.

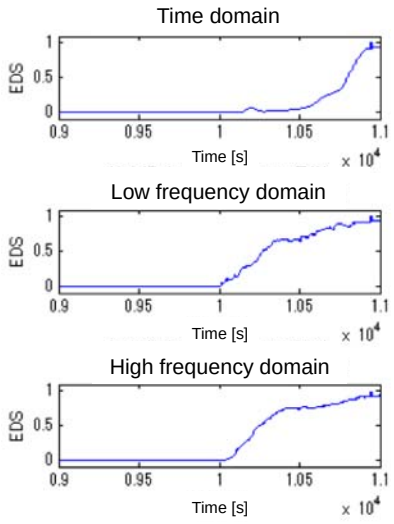

Fig. 11 Similarity indices to the normal operation case.

Figure 12 shows the trend graphs of similarity indices for four process signals at the anomaly case of a small decrease of feedwater temperature. As shown in this figure, similarity indices for three of the four process signals change from 1.0 to 0.0, implying the occurrence of an anomaly in the feedwater temperature since it decreases. This means that the technique can identify the anomaly that happened.

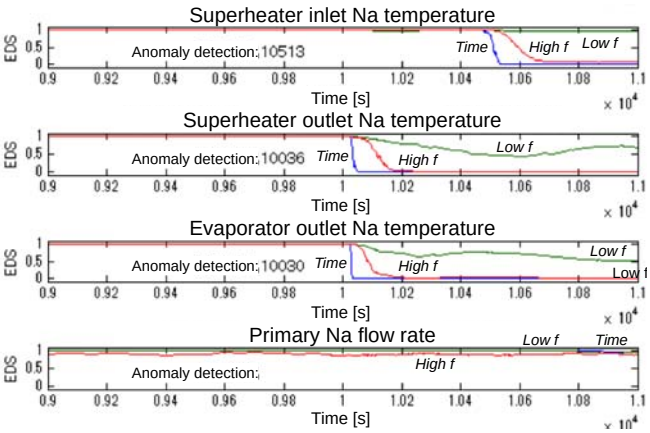

Fig. 12 Similarity indices to a case of small feedwater temperature decrease.

4 Hybrid diagnostic technique and its implementation as an agent system

The developed hybrid diagnostic system is shown in Fig. 13. It consists of the diagnosis integration sub-system and four diagnostic sub-systems. The principles and capabilities of the sub-systems are already described in the previous section.

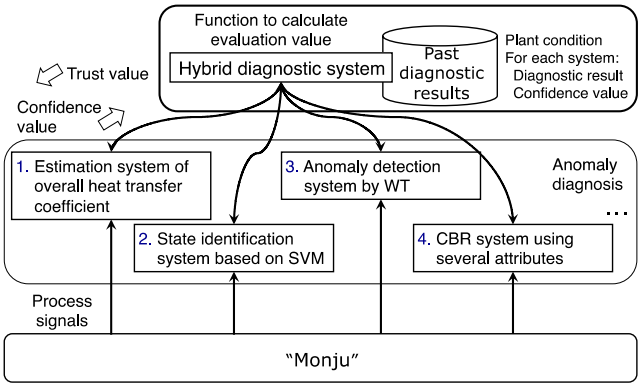

Fig. 13Hybrid diagnostic system.

To integrate the diagnostic results of sub-systems, each sub-system outputs its diagnostic result and confidence value for the result. The confidence value is given between 0.0 and 1.0. A confidence value of 1.0, means that the sub-system has absolute confidence. The diagnosis integration sub-system shown as “hybrid diagnostic system” in Fig. 13, gives an integrated diagnosis result by using predefined trust values for four diagnostic sub-systems. The trust value

is given between 0.0 and 1.0, and the value of 1.0 means that the diagnosis integration sub-system absolutely trusts the result of the corresponding diagnosis sub-system. The integrated diagnosis result is given to be a plant condition whose evaluation value is highest as calculated by the following equation:

$$E_i = \sum_J C_{Ji} \cdot T_{Ji} \qquad (11)$$

where E_i, C_{Ji}, and T_{Ji} are evaluation values for plant condition i, confidence value of sub-system J for plant condition i, and trust value for the diagnostic result of sub-system J in its diagnostic result of plant condition i.

The integration technique will be applicable to give a final diagnostic result based on the results of diagnostic sub-systems although further studies are necessary for the calculations of trust values. An approach based on the past diagnostic results and confidence values of diagnostic sub-systems will give reasonable trust values.

The diagnosis integration sub-system and four diagnostic sub-systems are implemented as an agent system of "Monju" distributed diagnostic agent system [1]. Figure 14 shows the relationship among "Monju" process data acquisition system MIDAS, some data servers, developed hybrid diagnostic agent, four developed diagnostic sub-agents, and other monitoring and diagnostic agents. The hybrid diagnostic agent corresponds to the diagnosis integration sub-system and calls a diagnostic sub-agent with necessary data to initiate the diagnostic process of the sub-agent. The sub-agent returns its diagnostic result and confidence value for the result to the hybrid diagnostic agent.

6 Concluding remarks

The article describes four diagnostic techniques and a hybrid diagnostic technique developed by the authors' four-year project. It also describes their implementation as an agent system for the "Monju" distributed diagnostic agent system.

Future works include the development of a technique to calculate the trust values for integrating the diagnostic results of sub-systems, applicability evaluations of the developed agent system through the condition monitoring of "Monju". Since an engineering plant has similar components akin to "Monju", it will be easy to apply the developed diagnostic techniques with some minor modifications to an engineering plant.

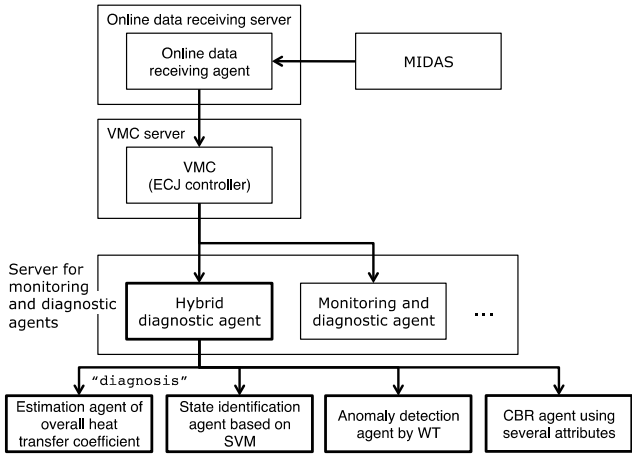

Fig. 14 Hybrid diagnostic agent as a subsystem of "Monju" distributed diagnostic agent system.

Acknowledgements

This study includes some of the results of "Anomaly detection agents by advanced hybrid processing of Monju process data" entrusted to Okayama University by the Ministry of Education, Culture, Sports, Science and Technology of Japan (MEXT). The authors are grateful to JAEA for providing the observed data of "Monju".

References

[1] TAMAYAMA, K., UDAGAWA, K., FUJINAMI, M., OKUSA, K., MURANAKA, M., KITAMURA, T., and MITSUMOTO, R.: Development of Distributed Plant Monitoring and Diagnosis System at "Monju", JNC Technical Review, 2001, No. 13: 5-12. (in Japanese)

[2] MOCHIZUKI, H.: Development of the Plant Dynamics Analysis Code NETFLOW++, Nuclear Engineering and Design, 2010, 240: 577-587.

[3] FURUSAWA, H., and GOFUKU, A.: Condition Monitoring of Steam Generator by Estimating the Overall Heat Transfer Coefficient, Int. J. Nuclear Safety and Simulation, 2013, 4 (1): 59-66.

[4] WIDODO, A., and YANG, B.-S.: Support Vector Machine in Machine Condition Monitoring and Fault Diagnosis. Mechanical Systems and Signal Processing, 2007, 21(6): 2560-2574.

[5] HUANG, C.-L., and WANG C.-J.: A GA-based Feature Selection and Parameters Optimization for Support Vector Machines, Expert Systems with Applications, 2006, 31 (2): 231–240.

[6] NAGAMATSU, T. , and GOFUKU, A.: Detection Method for Small Anomalies in Pumps Using Mother Wavelets Extracted from Real Vibration Signals, CD-ROM Proc. First Int. Symp. on Socially and Technically Symbiotic Systems, 01STSS2012-16.pdf, 2012.

[7] ZHANG, Z., IKEUCHI, H., SAIKI, N., IMAMURA, T., ISHII, H., TODA, H., and MIYAKE, T., Parasitic Discrete Wavelet Transform and Its Application on Abnormal Signal Detection, Transactions of the JSME (C), 2009, 75 (757): 163-170. (in Japanese)

[8] DIANTONO, C., TAKAHASHI, M., and KITAMURA, M.: Symptom Database for Intelligent Detection and Characterization of Incipient Failures in Nuclear Power Plant, Proc. Maintenance and Reliability Conf. MARCON98, 1, 24.01-24.08, 1998.